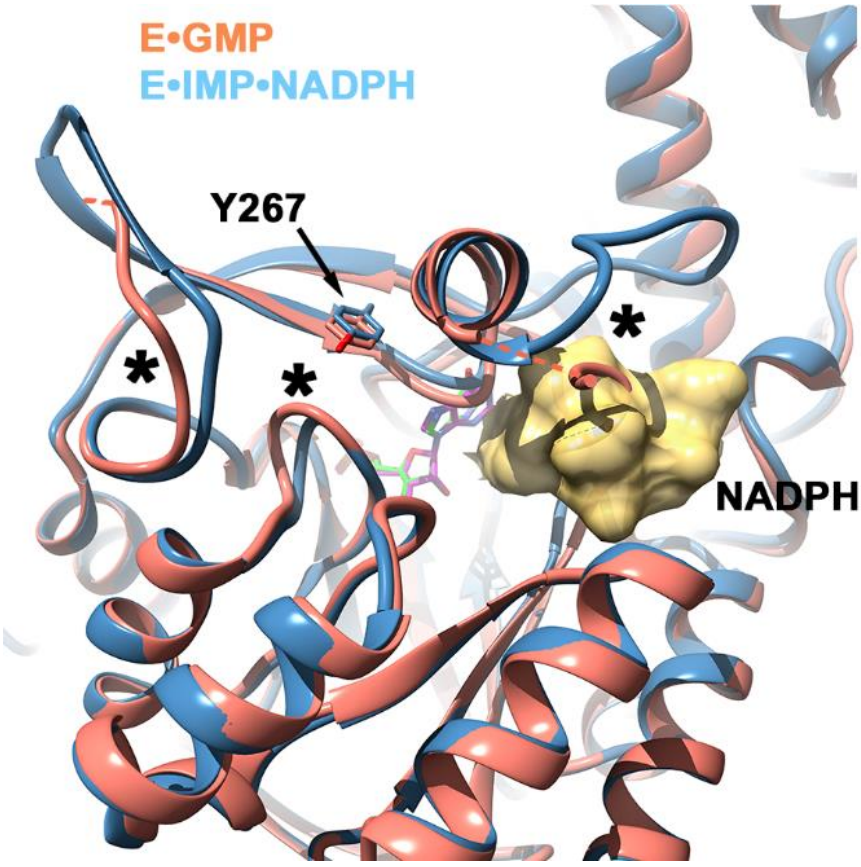

Figure S1. Location of tyrosine 267 near GMPR active site, related to Fig. 1

The active site of the E•GMP complex of human GMPR is shown in orange (PDB id: 2BLE), the E•IMP•NADPH complex of human GMPR2 is shown in blue (PDB id: 22C6Q). Tyr267 is shown as sticks, IMP is shown in green sticks, GMP in magenta sticks and NADPH is a gold surface. Asterisks denote regions of conformational change. Note that a mobile loop occludes the NADPH binding site in the E•GMP complex.

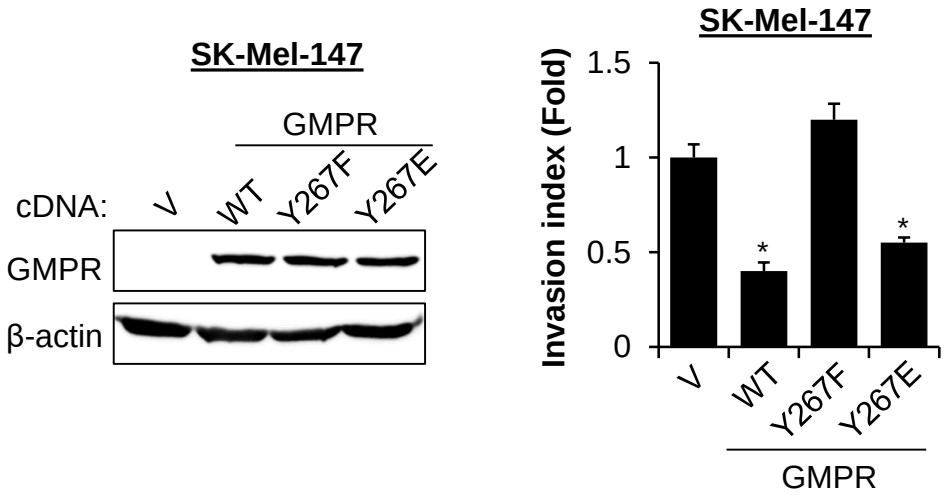

Figure S2. Phosphorylation of tyrosine 267 is critical for GMPR activity, related to Fig. 2

SK-Mel-147 cells transduced with empty lentivirus vector (V) or vectors expressing cDNA encoding the indicated FLAG-tagged GMPR mutants (GMPR) were probed in immunoblotting with the indicated antibodies (left) or evaluated Boyden's chamber invasion assay. Data represent average +/- SEM from ≥ 2 biological replicas, Student's t-test.

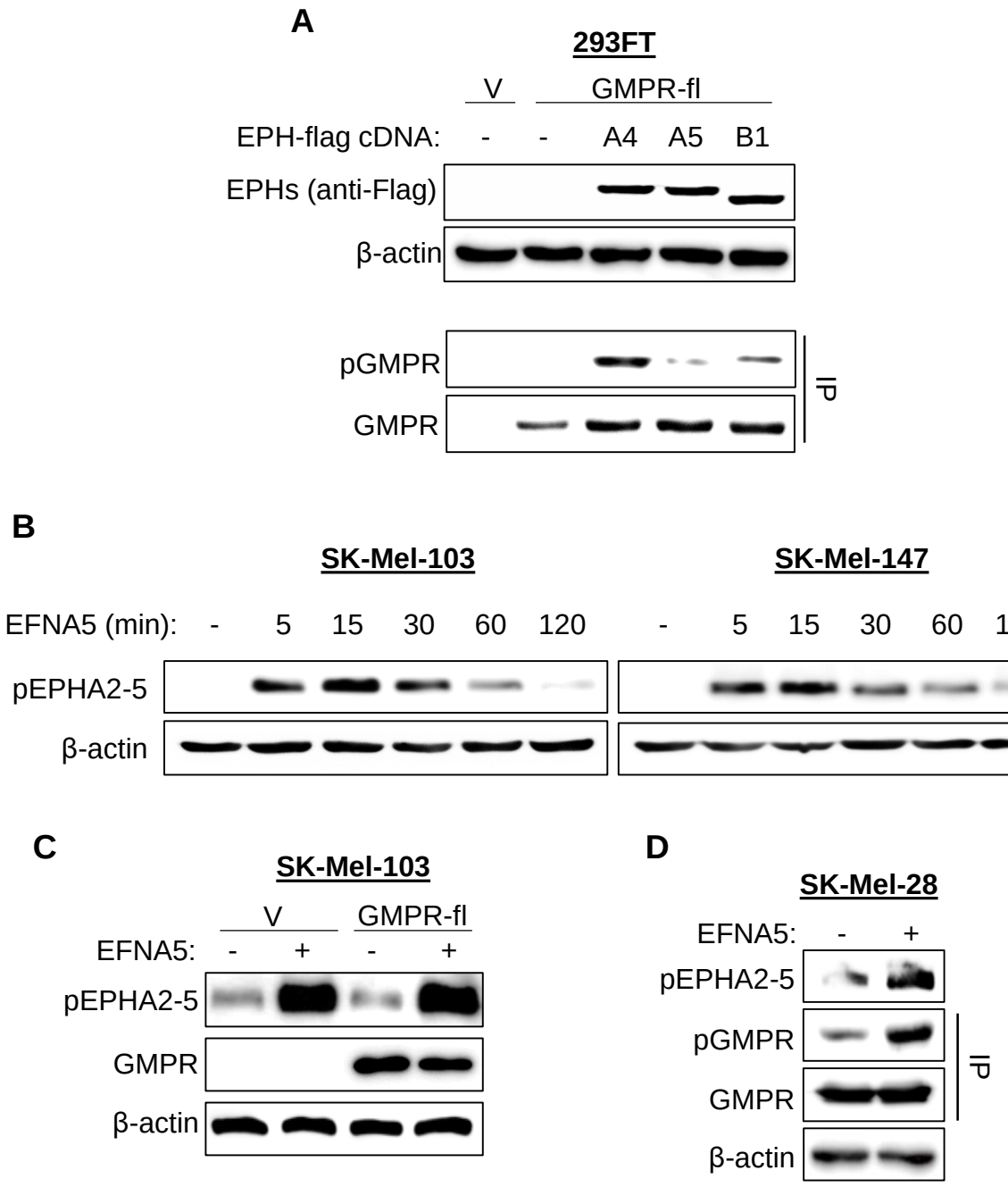

Figure S3. The EFNA5-EPHA4 axis drives GMPR^{Y267} phosphorylation in melanoma cells, related to Fig. 3

A. 293FT cells were co-transfected with the empty vector (V) or vectors expressing the indicated cDNA (GMPR, EPHA4 (A4), EPHA5 (A5), EPHB1 (B1)). Cells were probed in immunoblotting with the indicated antibodies (top) or immunoprecipitated with anti-FLAG antibodies followed by immunoblotting with the indicated antibodies (bottom). **B.** Melanoma cells were treated with soluble EFNA5 (2µg/mL) for the indicated time intervals followed by immunoblotting with the indicated antibodies. **C.** SK-Mel-103 cells transduced with control or GMPR-expressing lentivirus were treated with or without EFNA5 (2 µg/mL for 30 minutes) followed by immunoblotting with the indicated antibodies. **D.** SK-Mel-28 cells were treated with or without EFNA5 as in (C) and probed in immunoblotting with indicated antibodies or immunoprecipitated with anti-GMPR antibodies and probed as indicated.

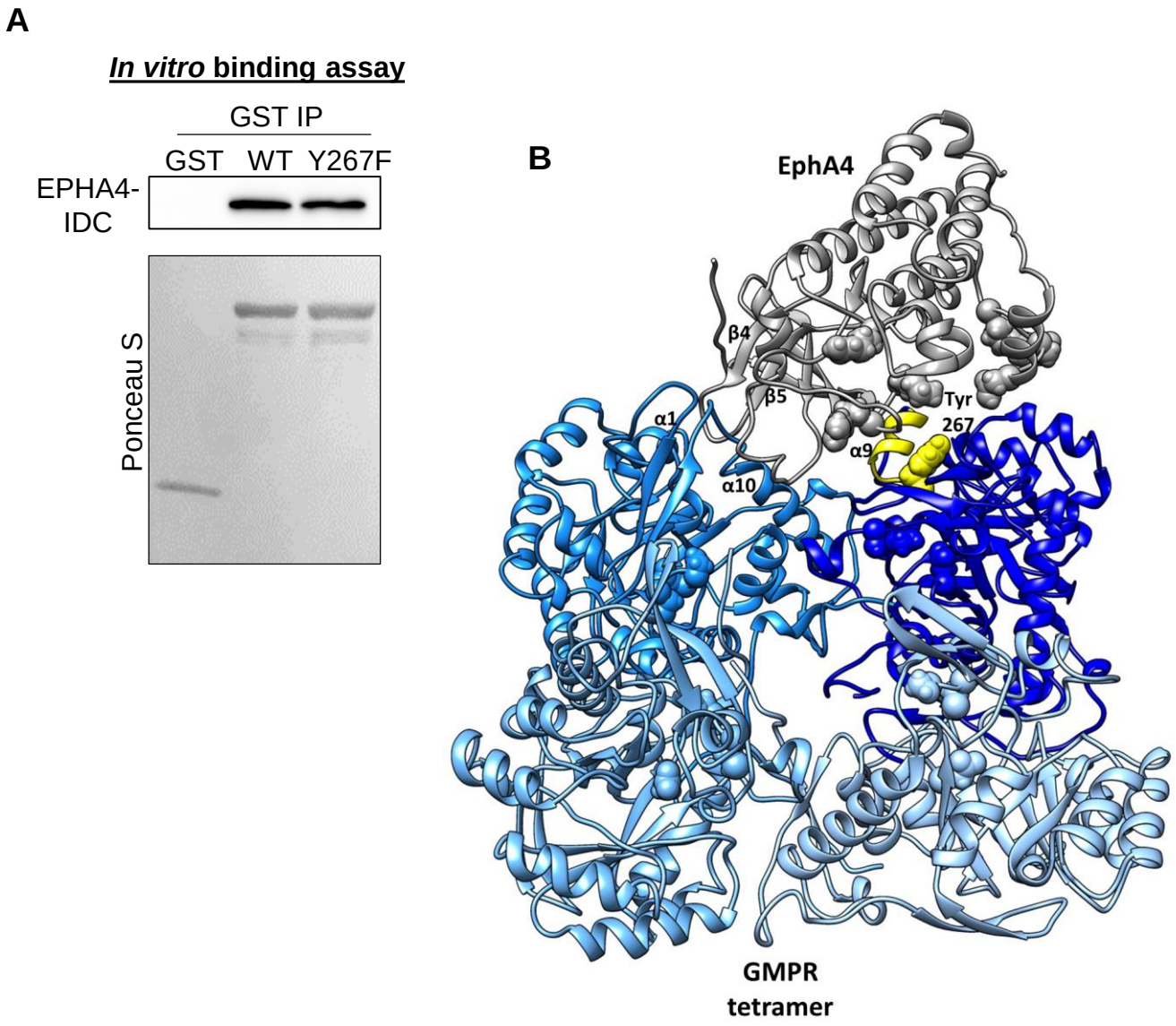

Figure S4. Modeled potential GMPR-EPHA4 complex, related to Fig. 4
A. Bacterially purified GST-tagged GMPR or GMPR^{Y267F} was probed in an *in vitro* binding assay with purified EPHA4, and analyzed in immunoblotting with the indicated antibody or via Ponceau S staining. **B.** Angled top view of the proposed interaction between EPHA4 (gray) and the GMPR tetramer (blue). The GMPR Tyr 267 phosphorylation site (yellow) is in a helix prone to disorder (shown in yellow ribbon, α9), and interacts with the substrate binding site of EPHA4 (key residues shown in space-filling representation), with the interaction stabilized by residues from a neighboring GMPR monomer, primarily via interactions with the α10 helix.

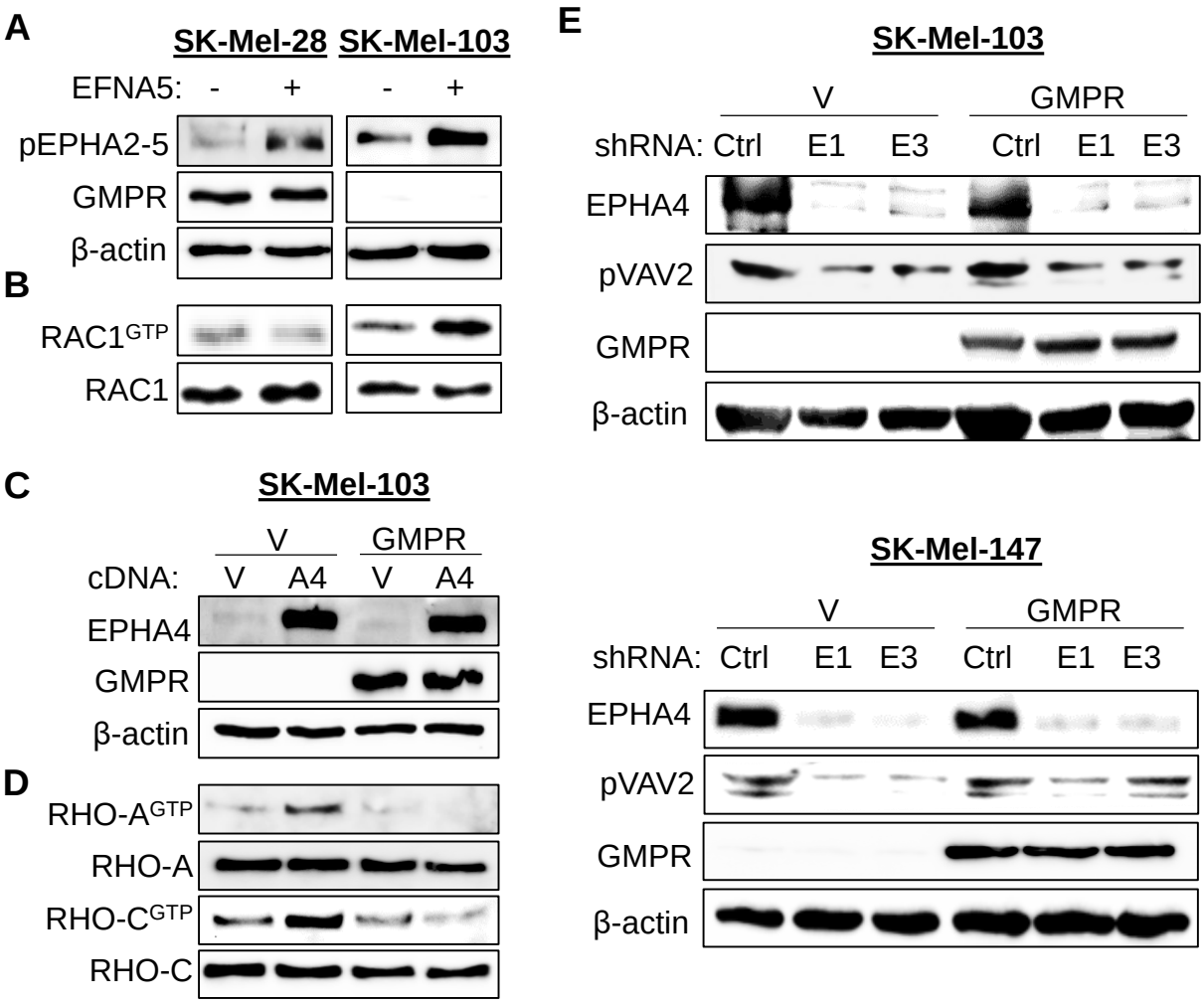

Figure S5. Phosphorylation of GMPR by EFNA5-EPHA4 axis influences RHO-GTPase activation, related to Fig. 7

A. SK-Mel-28 and SK-Mel-103 cells were treated or not with 2 µg/mL EFNA5 for 30 minutes prior to harvesting. PBS was used as a vehicle control. Cells were probed in immunoblotting with the antibodies indicated. **B.** Cells described in (A) were probed in RAC1 activity pulldown assay followed by immunoblotting. **C.** SK-Mel-103 cells transduced with the indicated constructs (V, GMPR, EPHA4) were probed in immunoblotting with the indicated antibodies. **D.** Cells described in (C) were probed in RHO GTPase activity pulldown assay followed by immunoblotting. **E.** Cells were transduced with the indicated constructs (empty vector (pLV), GMPR, Ctrl - control shRNA, E1 - EPHA4 shRNA1, E3 – EPHA4 shRNA3) and probed in immunoblotting with the indicated antibodies.

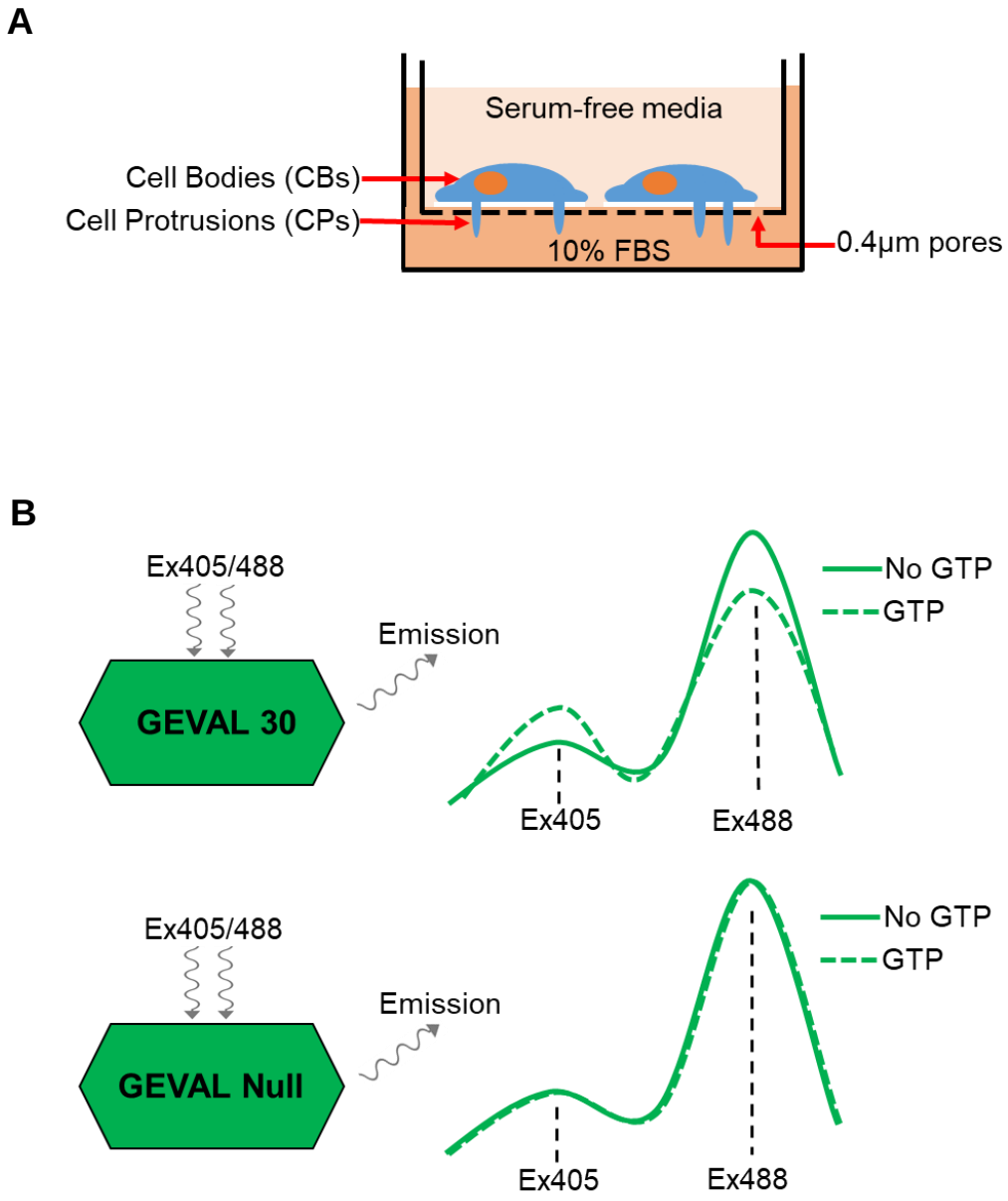

Figure S6. Schematics of cell body vs. cell protrusion fractionation and GEVAL activities, related to Fig. 7

A. Schematic representation of the chamber used for separation of cell bodies (CBs) and cell protrusions (CPs). **B.** Schematic representation of GEVALs used for visualizing intracellular GTP.

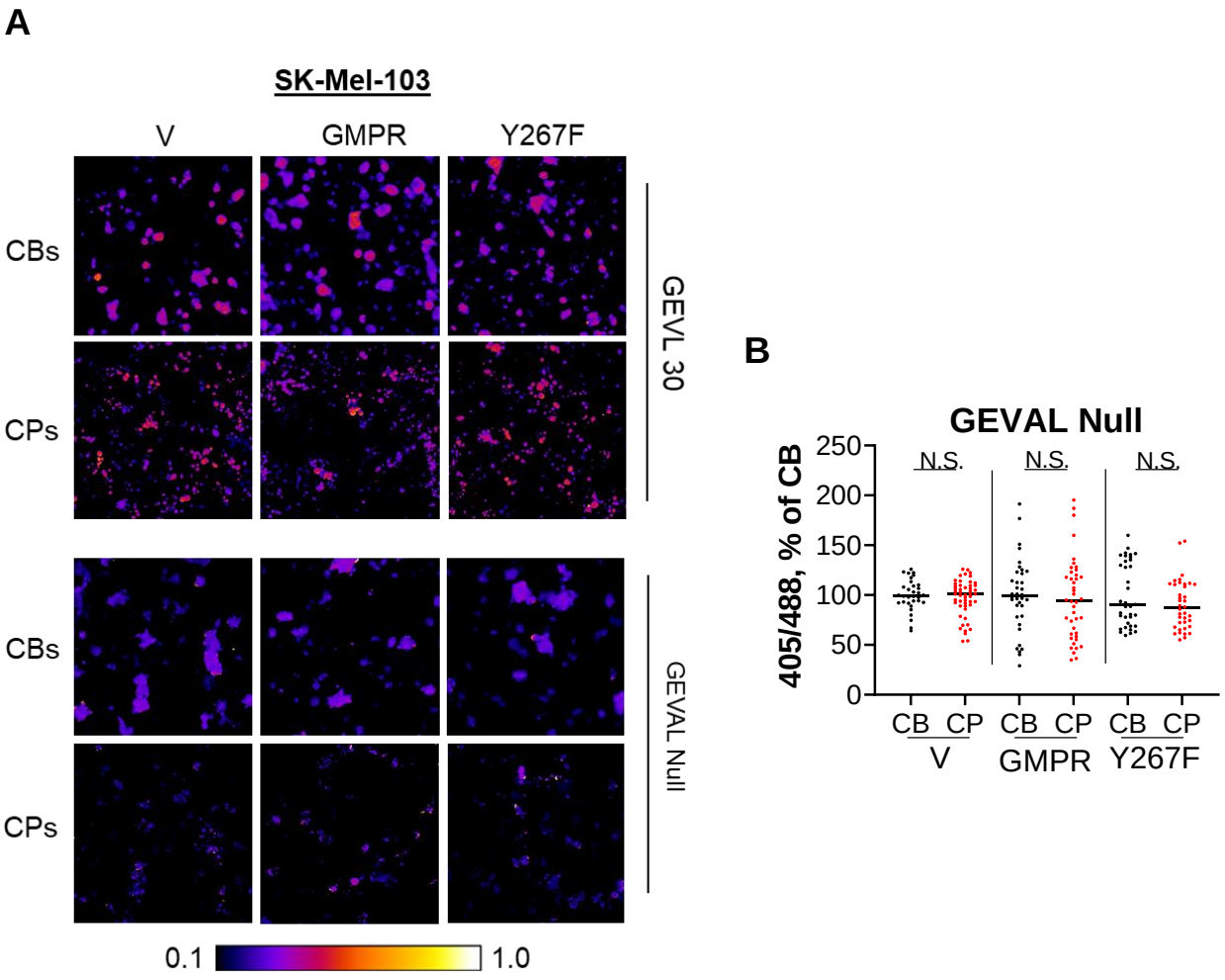

Figure S7. GMPR suppresses GTP levels in cell protrusions, related to Fig. 7

A. SK-Mel-103 cells stably expressing the indicated constructs (control vector - V, GMPR, GMPR^{Y267F}) were probed in GEVAL activity assays as described in Materials and Methods. Representative false-colored radiometric images of cell bodies and cell protrusions in cells transduced with GEVAL 30 or GEVAL Null. **B.** Shown is dot-plot quantification of GEVAL activity in CBs and CPs of the indicated cells. Bars represent the mean value as a percentage of CB signal for each condition. Statistical analysis was performed by using the Mann-Whitney *U* test.

In vitro kinase screen

Kinase	With peptide	Without peptide	Activity ratio
EPHA5	33	0	N/A
VEGF-R3	38	0	N/A
TRK-C	54	1	38.00
FER	120	24	4.33
EPHA4	250	61	3.84
KIT	41	9	2.78
EPHA6	92	28	2.71
FGF-R1	200	76	2.42
EPHB1	82	28	2.36
TIE2	48	15	2.13

Table S1. *In vitro* kinase screen reveals EPHs as potentially phosphorylating GMPR^{Y267}, related to Fig. 3

Indirect ELISA

Antibody concentration (ng/mL)	pGMPR peptide	GMPR peptide
1000.00	3.622	0.242
500.00	3.426	0.148
250.00	3.313	0.134
125.00	3.069	0.118
62.50	2.805	0.111
31.25	2.361	0.102
15.62	1.658	0.098
7.81	0.967	0.091
3.90	0.493	0.089
1.95	0.265	0.086
blank	0.060	0.096
blank	0.060	0.096

Table S2. ELISA assay confirms specificity of anti-phospho-GMPR^{Y267} antibody, related to Fig. 3

In vitro GMPR activity assay

Enzyme	V_{max}, nM/s		K_m(NADPH), μM		K_m(GMP), μM
	Best fit ± std	95% CI	Best fit ± std	95% CI	Upper limit
GMPR	1.79 ± 0.07	1.61 to 1.99	13.4 ± 1.9	8.80 to 20.0	≤ 19
pGMPR	3.60 ± 0.18	3.13 to 4.17	18.3 ± 3.1	10.9 to 30.0	≤ 23

Table S3. Steady-state kinetic parameters for recombinant GST-GMPR and GST-pGMPR, related to Fig. 4F. Enzymes were incubated with saturating fixed concentration of GMP (100 μM) and varying concentrations of NADPH (6.25-100 μM) to determine V_{max} and K_m(NADPH). To determine K_m(GMP), enzyme was incubated with fixed NADPH (100 μM) and varying concentrations of GMP (25-150 μM). The best fit and standard deviation to the Michaelis-Menton equation and 95% confidence limits (CI) are reported. Only an upper limit could be obtained for K_m(GMP).